

Date of publication Month Day, 2020, date of current version Month Day, 2020.

Digital Object Identifier 10.1109/ACCESS.2020.DOI

Effective Throughput Analysis of α - η - κ - μ Fading Channels

YUN AI^{1*}, (Member, IEEE), AASHISH MATHUR^{2*}, (Member, IEEE),
LONG KONG³, (Member, IEEE), and MICHAEL CHEFFENA¹

¹Faculty of Engineering, Norwegian University of Science and Technology, 2815 Gjøvik, Norway (e-mails: yun.ai@ntnu.no, michael.cheffena@ntnu.no)

²Department of Electrical Engineering, Indian Institute of Technology Jodhpur, 342037 Jodhpur, India (e-mail: aashishmathur@iitj.ac.in)

³Interdisciplinary Centre for Security, Reliability and Trust, University of Luxembourg, L-1855 Luxembourg (e-mail: long.kong@uni.lu)

*The authors contribute equally to this work.

Corresponding author: Yun Ai

ABSTRACT The α - η - κ - μ fading model is a very useful instrument to accurately describe various radio wave propagation scenarios. In this paper, we study the effective throughput performance of communication systems over the α - η - κ - μ fading channels. Novel and exact expressions for the effective throughput over α - η - κ - μ channels are derived, and the effective throughput of multiple-input single-output (MISO) and multiple-input multiple-output (MIMO) systems over some widely used small-scale fading models are presented based on the derived results. To obtain more understandings on the impact of physical channel characteristics and system configuration on the effective throughput, closed-form expressions for the asymptotic effective throughput at high signal-to-noise ratio (SNR) regimes are also obtained. The results reveal the underlying connections between different physical channel parameters (e.g., scattering level, phase correlation, channel nonlinearity, multipath clustering, and channel imbalance) and the effective throughput. It is found that the effective throughput improves with the increase of channel nonlinearity and number of multipath clusters, and the high-SNR slope is only dependent on the channel nonlinearity and the number of multipath clusters present in the physical channel.

INDEX TERMS Effective throughput, quality-of-service (QoS), α - η - κ - μ fading channels, generalized fading, multiple-input single-output (MISO), multiple-input multiple-output (MIMO).

I. INTRODUCTION

The well-established Shannon ergodic capacity was derived under the assumption that there exists no delay for the communication system. In order to describe the practical communication service process and to evaluate the system performance under the quality-of-service (QoS) requirements such as system delay, reliability, and energy efficiency, the concept of effective throughput (a.k.a. effective capacity and effective rate) was proposed in [1]. In the context of effective throughput, the maximum constant arrival rate at the transmitter is measured when guaranteed statistical delay constraints are assumed to be present [1]–[3].

The effective throughput performance analysis over various fading channels and communication configurations have been conducted to accommodate the performance analysis of different communication scenarios under realistic constraints [4]–[12]. The effective capacity over κ - μ and Fisher-Snedecor \mathcal{F} fading channels were studied in [4] and [5], respectively. In [6], the effective rate analysis over composite

α - η - μ /gamma fading channel was conducted by approximating the fading distribution with mixture Gamma (MG) and mixture of Gaussian (MoG) models. The effective rate performance of multiple-input single-output (MISO) systems over Generalized K and α - μ channels were respectively studied in [7] and [8]. The power allocation scheme to maximize the effective capacity of a virtual multiple-input multiple-output (MIMO) system was studied in [9]. The closed-form analytical expressions for the effective capacity of the nonorthogonal multiple access (NOMA) fading channels was derived in [10]. The effective capacity of ultra reliable machine-type communications is analyzed in [11] by including the effects of power allocation. The combined implementation of the automatic repeat request (ARQ) at link layer and adaptive modulation to improve the effective throughput of wireless communication system was proposed and investigated in [12].

Recently, a novel fading model named α - η - κ - μ distribution has been developed in [13]. The α - η - κ - μ fading distribu-

tion is arguably the most versatile and comprehensive model in research literature as it includes the extensively used fading models such as α - μ , κ - μ , Rayleigh, Beckmann, Nakagami- m , Rice, Hoyt, and Weibull distributions as its special cases [13]–[15]. More importantly, the new model is developed on a physical basis, which provides valuable flexibility and versatility to adapt different behaviors from various propagation scenarios. For instance, the model takes into account of the effects of nonunimodality and imbalance between in-phase and quadrature signals, which are seen from a number of new wireless propagation scenarios as detailed in [13]. The versatility of the model makes it useful for accurate modeling of the channels, where the well-established models cannot accurately describe [13]–[19]. As an instance, from extensive millimeter wave (mmWave) channel measurements (e.g., outdoor line-of-sight (LoS) and non-LoS (NLoS) scenarios at 28 GHz and indoor LoS scenario at 60 GHz [14]), it was observed that the α - η - κ - μ model fits the mmWave measurements best. Another appealing point of this physical basis in developing the model is that it enables to comprehend and investigate the connections between the evaluated performance metrics and physical channel characteristics (e.g., scattering level, channel nonlinearity, phase correlation, multipath clustering, etc.) straightforwardly.

Despite the many advantages of the α - η - κ - μ model, to the best of authors' knowledge, the effective throughput performance of communication systems over this useful fading channel has not been investigated yet. The α - η - κ - μ model has the great potential in various emerging scenarios, especially in mmWave communication. It is well known that mmWave communication will play a significant role in the next generation of communication system (5G and beyond) featuring extreme low latency and high reliability. Motivated by the above facts, we investigate the effective throughput performance of wireless systems over α - η - κ - μ fading channels by deriving the exact expression of effective throughput and conducting asymptotic analysis in this paper.

The remaining part of the paper is structured as follows. In Section II, we first describe the α - η - κ - μ fading model followed by the theoretical effective throughput analysis. Based on the derived results, the effective throughput of multi-antenna system over some certain small-scale fading channels are also presented in Section II, where the asymptotic analysis is also performed to get more insights on the impact of physical channel parameters on the effective throughput. The analytical and simulation results are given and elaborated in Section III. Section IV summarizes the paper.

Notations: $(\cdot)_n$ is the Pochhammer symbol [20, p. 800], $L_b^a(\cdot)$ denotes the Laguerre polynomial [20, p. 795], $\Gamma(\cdot)$ is the Gamma function [20, p. 797], $E[\cdot]$ represents the expectation operation, $G_{p,q}^{m,n}(\cdot|\cdot)$ and $H_{p,q}^{m,n}(\cdot|\cdot)$ are respectively the Meijer G-function [20] and Fox H-function [21], $H_{p,q;t,u;v,w,x}^{m,n:r,s:v,u}(\cdot)$ is the extended generalized bivariate Fox H-function (EGBFHF) that can be evaluated with numerical softwares such as Matlab and Mathematica [22], $B(\cdot, \cdot)$ denotes the Beta function [23, Eq. (8.38)], and $\|\mathbf{H}\|_F$ represents

the Frobenius norm (a.k.a. Euclidean norm) of the matrix \mathbf{H} [24, p. 60].

II. EFFECTIVE THROUGHPUT ANALYSIS

A. THE α - η - κ - μ FADING MODEL

When the channel fading coefficient h is a random variable (RV) that follows the α - η - κ - μ fading distribution, the corresponding probability density function (PDF) can be written as [13]:

$$f_h(x) = \frac{\alpha x^{\alpha\mu-1} e^{-\left(\frac{x^\alpha}{2}\right)} \sum_{k=0}^{\infty} \frac{k! c_k}{(\mu)_k} L_k^{\mu-1}(2x^\alpha). \quad (1)$$

The PDF in (1) is underpinned by the parameters α , η , κ , μ , p , and q , where α describes the severity of the channel nonlinearity, η is the ratio between the in-phase component power and the quadrature component power of the scattered waves, κ signifies the ratio of the dominant components power to the scattered waves power, μ represents the multipath cluster number, the imbalance parameter p denotes the ratio of the multipath cluster numbers of in-phase and quadrature components, and another imbalance parameter q is given as the ratio of two proportions: the ratio of the dominant components power to the scattered waves power of the in-phase components and its counterpart for the quadrature components [14]. The parameter c_k in (1) is obtained with the parameters α , η , κ , μ , p , and q by utilizing the recursive equation given by [13, Eq. (15)] and the relations in [13, Eqs. (30) and (31)]. It should be noted that despite the expression for the PDF of α - η - κ - μ RV in (1) consists of infinite number of terms, it converges fast only with limited terms [17].

The instantaneous signal-to-noise ratio (SNR) γ at the receiver can be expressed as

$$\gamma = \frac{E_s \cdot h^2}{N_0} = \bar{\gamma} \cdot h^2, \quad (2)$$

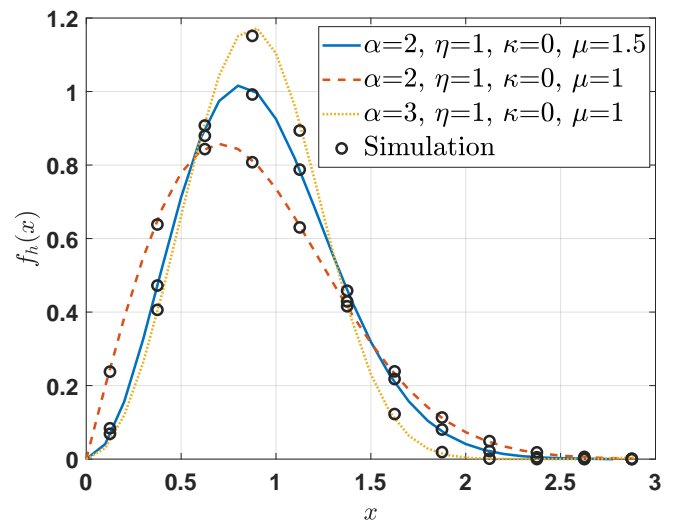


FIGURE 1. Simulation and analytical results of fading PDF in (1) with $k = 10$ terms

where E_s is the transmitted signal energy, N_0 is the power spectral density of the additive white Gaussian noise (AWGN) at the corresponding receiver, and $\bar{\gamma} = \frac{E_s}{N_0}$.

Utilizing the relationship in (2) and following the expression given in (1), the PDF of the SNR γ over α - η - κ - μ fading channel with $\bar{\gamma}$ being the average SNR is expressed as [15]

$$f_\gamma(x) = \frac{\alpha}{2^{\mu+1} \cdot \Gamma(\mu) \cdot \bar{\gamma}^{\frac{\alpha\mu}{2}}} \cdot x^{\frac{\alpha\mu}{2}-1} \cdot \exp\left(-\frac{x^{\frac{\alpha}{2}}}{2\bar{\gamma}^{\frac{\alpha}{2}}}\right) \cdot \sum_{k=0}^{\infty} \frac{k!c_k}{(\mu)_k} L_k^{\mu-1}\left(2\left(\frac{x}{\bar{\gamma}}\right)^{\frac{\alpha}{2}}\right). \quad (3)$$

It should be noted that although the PDFs in Eq. (1) and Eq. (3) are expressed in terms of infinite series, the series converge for finitely small value of k . This is also justified by the close matching of the analytical and simulation results. For instance, $k = 10$ is sufficient for the convergence of the series for the parameter values as demonstrated in Figure 1 at the bottom of previous page.

B. EFFECTIVE THROUGHPUT ANALYSIS

Assuming that the data reaches the buffer over block fading channel at fixed rate and the service process is stationary, the normalized effective throughput (in bits/s/Hz) of the communication channel is defined as [25], [26]

$$\mathcal{R} = -\frac{1}{A} \cdot \log_2(\mathbb{E}[(1 + \gamma)^{-A}]), \quad (4)$$

where $A = \theta TB / \ln 2$ with θ , T , and B being the delay exponent, block duration, and system bandwidth, respectively. More specifically, the delay exponent θ is related to the probability that the equilibrium queue length l at the transmitter buffer exceeds some specific threshold L as follows [8]:

$$\theta = -\lim_{L \rightarrow \infty} \frac{1}{L} \cdot \ln(\Pr(l > L)). \quad (5)$$

It is clear from (4) and (5) that the effective throughput is dependent on both the statistics of the fading channel as well as the system configuration. When there exists no constraint on delay requirement, i.e., $\Pr(l > L) \rightarrow 0$ and thus $\theta \rightarrow 0$, the effective throughput becomes equivalent to the Shannon's ergodic capacity of the corresponding fading channel.

Using (3) and (4), the exact expression for the effective throughput of communication systems over the investigated α - η - κ - μ fading channel is obtained as

$$\begin{aligned} \mathcal{R}(\bar{\gamma}, \theta) &= -\frac{1}{A} \cdot \log_2\left(\int_0^\infty (1+x)^{-A} \cdot f_\gamma(x) dx\right) \\ &= -\frac{1}{A} \cdot \log_2\left(\frac{\alpha}{2^{\mu+1}\Gamma(\mu)\bar{\gamma}^{\frac{\alpha\mu}{2}}} \cdot \sum_{k=0}^{\infty} \frac{k!c_k}{(\mu)_k} \cdot \mathcal{I}\right), \end{aligned} \quad (6)$$

where

$$\mathcal{I} = \int_0^\infty \frac{x^{\frac{\alpha\mu}{2}-1}}{(1+x)^A} \exp\left(\frac{-x^{\frac{\alpha}{2}}}{2\bar{\gamma}^{\frac{\alpha}{2}}}\right) L_k^{\mu-1}\left(2\left(\frac{x}{\bar{\gamma}}\right)^{\frac{\alpha}{2}}\right) dx. \quad (7)$$

In the following, we find an analytical and exact solution to the above integral \mathcal{I} in (7). We first make use of the following

transformations between the relevant elementary functions and the Meijer G-function [20, Chpt. 8.4]:

$$(1+x)^{-a} = \frac{1}{\Gamma(a)} \cdot G_{1,1}^{1,1}(x|_{1-a}^{-a}), \quad (8a)$$

$$\exp(-ax) = G_{0,1}^{1,0}(ax|_{-}), \quad (8b)$$

$$L_b^a(x) = \frac{\exp(x)}{\Gamma(b+1)} \cdot G_{1,2}^{1,1}(x|_{0,-a}^{-a-b}). \quad (8c)$$

Expressing the relevant functions in (7) in terms of the Meijer G-functions with the aid of (8), the integral in (7) can be alternatively expressed as

$$\begin{aligned} \mathcal{I} &= \int_0^\infty \frac{x^{\frac{\alpha\mu}{2}-1}}{\Gamma(A)\Gamma(k+1)} \cdot G_{1,1}^{1,1}(x|_{1-A}^{1-A}) \cdot G_{1,2}^{1,0}\left(\frac{3x^{\frac{\alpha}{2}}}{2\bar{\gamma}^{\frac{\alpha}{2}}}\middle|\frac{1}{2}, \frac{1}{2}\right) \\ &\quad \cdot G_{1,2}^{1,1}\left(\frac{2x^{\frac{\alpha}{2}}}{\bar{\gamma}^{\frac{\alpha}{2}}}\middle|_{0,1-\mu}^{1-\kappa-\mu}\right) dx. \end{aligned} \quad (9)$$

Subsequently, rewriting the Meijer G-functions in (9) in Fox H-functions utilizing the following relationship between the two functions [20, Eq. (8.3.2.21)], i.e.,

$$G_{p,q}^{m,n}\left(x\middle|\begin{smallmatrix} \mathbf{a}_p \\ \mathbf{b}_q \end{smallmatrix}\right) = H_{p,q}^{m,n}\left(x\middle|\begin{smallmatrix} (\mathbf{a}_p, 1) \\ (\mathbf{b}_q, 1) \end{smallmatrix}\right), \quad (10)$$

and then conducting a change of RV: $x^{\frac{\alpha}{2}} \rightarrow x$, further solving the resultant integral with the property [27, Eq. (2.3)], the considered integral can be solved as the following closed-form solution in terms of the EGBFHF:

$$\begin{aligned} \mathcal{I} &= \frac{2\pi}{\alpha\Gamma(A)\Gamma(k+1)} \cdot \int_0^\infty x^{\mu-1} \cdot H_{1,2}^{1,1}\left(\frac{2x}{\bar{\gamma}^{\frac{\alpha}{2}}}\middle|\begin{smallmatrix} (1-\kappa-\mu, 1) \\ (0, 1), (1-\mu, 1) \end{smallmatrix}\right) \\ &\quad \cdot H_{1,1}^{1,1}\left(x^{\frac{2}{\alpha}}\middle|\begin{smallmatrix} (1-A, 1) \\ (0, 1) \end{smallmatrix}\right) \cdot H_{1,2}^{1,0}\left(\frac{3x}{2\bar{\gamma}^{\frac{\alpha}{2}}}\middle|\begin{smallmatrix} (\frac{1}{2}, 1) \\ (0, 1), (\frac{1}{2}, 1) \end{smallmatrix}\right) dx \\ &= \frac{2^{\mu+1}3^{-\mu}\pi\bar{\gamma}^{\frac{\alpha\mu}{2}}}{\alpha\Gamma(A)\Gamma(k+1)} \cdot H_{2,1:1:1:1,2}^{0,1:1:1:1,2}\left(\mathcal{K}_{1a}\middle|\mathcal{K}_{2a}\mathcal{K}_{3a}\middle|\frac{2\frac{\alpha}{2}\bar{\gamma}^{\frac{3}{\alpha}}}{3\frac{\alpha}{2}}, \frac{4}{3}\right), \end{aligned} \quad (11)$$

where $\mathcal{K}_{1a} = (1-\mu; \frac{2}{\alpha}, 1)$, $(\frac{1}{2}-\mu; \frac{2}{\alpha}, 1)$; $\mathcal{K}_{2a} = (1-A, 1)$; $\mathcal{K}_{2b} = (0, 1)$; $\mathcal{K}_{3a} = (1-\kappa-\mu, 1)$; and $\mathcal{K}_{3b} = (0, 1), (1-\mu, 1)$.

Substituting (11) into (6) and after some simple algebraic operations, we obtain the novel and exact expression for the effective throughput of wireless systems over α - η - κ - μ fading as shown in (12) at the top of next page.

C. SPECIAL CASES

Due to the fact that a large number of conventional fading distributions can be obtained as the special cases of the α - η - κ - μ model, the derived expression for effective throughput in (12) is highly generalized and can be straightforwardly expanded to the expressions of effective throughput over other fading channels with appropriate parameter mapping. Parameterization of some special cases of the α - η - κ - μ fading model is listed in Table 1, which also includes the empirical extracted parameters from some mmWave channel measurements at 28 GHz and 60 GHz [14].

Observing Table 1, it can be seen that the conventional models all assume balance between in-phase and quadrature

$$\mathcal{R}(\bar{\gamma}, \theta) = -\frac{1}{A} \cdot \log_2 \left(\frac{\pi}{3^\mu \Gamma(A) \Gamma(\mu)} \cdot \sum_{k=0}^{\infty} \frac{c_k}{(\mu)_k} \cdot H_{2,1:1,1:1,1,2}^{0,1:1,1:1,1,1} \left(\mathcal{K}_{1a} \mid \mathcal{K}_{2a} \mid \mathcal{K}_{3a} \mid \frac{2^{\frac{2}{\alpha}} \bar{\gamma}^{\frac{3}{\alpha}}}{3^{\frac{2}{\alpha}}}, \frac{4}{3} \right) \right). \quad (12)$$

$$\mathcal{R}^{\text{MIMO, Rayleigh}}(\bar{\gamma}, \theta) = -\frac{1}{A} \cdot \log_2 \left(\frac{\pi}{3^{N_t N_r} \Gamma(A) \Gamma(N_t N_r)} \cdot \sum_{k=0}^{\infty} \frac{c_k}{(N_t N_r)_k} \cdot H_{2,1:1,1:1,1,2}^{0,1:1,1:1,1,1} \left(\mathcal{K}_{1a} \mid \mathcal{K}_{2a} \mid \mathcal{K}_{3a} \mid \frac{2^{\frac{2}{\alpha}} \bar{\gamma}^{\frac{3}{\alpha}}}{3^{\frac{2}{\alpha}}}, \frac{4}{3} \right) \right). \quad (15)$$

$$\mathcal{R}^{\text{MISO, Nakagami-}m}(\bar{\gamma}, \theta) = -\frac{1}{A} \cdot \log_2 \left(\frac{\pi}{3^{m N_t} \Gamma(A) \Gamma(m N_t)} \cdot \sum_{k=0}^{\infty} \frac{c_k}{(m N_t)_k} \cdot H_{2,1:1,1:1,1,2}^{0,1:1,1:1,1,1} \left(\mathcal{K}_{1a} \mid \mathcal{K}_{2a} \mid \mathcal{K}_{3a} \mid \frac{2^{\frac{2}{\alpha}} \bar{\gamma}^{\frac{3}{\alpha}}}{3^{\frac{2}{\alpha}}}, \frac{4}{3} \right) \right). \quad (16)$$

$$\mathcal{R}^{\text{MISO, } \alpha\text{-}\mu}(\bar{\gamma}, \theta) = -\frac{1}{A} \cdot \log_2 \left(\frac{\pi}{3^{\tilde{\mu}} \Gamma(A) \Gamma(\tilde{\mu})} \cdot \sum_{k=0}^{\infty} \frac{c_k}{(\tilde{\mu})_k} \cdot H_{2,1:1,1:1,1,2}^{0,1:1,1:1,1,1} \left(\mathcal{K}_{1a} \mid \mathcal{K}_{2a} \mid \mathcal{K}_{3a} \mid \frac{2^{\frac{2}{\alpha}} \bar{\gamma}^{\frac{3}{\alpha}}}{3^{\frac{2}{\alpha}}}, \frac{4}{3} \right) \right). \quad (17)$$

TABLE 1. Selected Special Cases of the $\alpha\text{-}\eta\text{-}\kappa\text{-}\mu$ Fading Model and Field Measurements [13]

Fading	$(\alpha, \eta, \kappa, \mu, p, q)$
$\alpha\text{-}\mu$	$(\alpha, 1, 0, \mu, 1, 1)$
Rayleigh	$(2, 1, 0, 1, 1, 1)$
$\kappa\text{-}\mu$	$(2, 1, \kappa, \mu, 1, 1)$
Rician	$(2, 1, K, 1, 1, 1)$
Beckmann	$(2, \eta, \kappa, 1, 1, 1)$
Nakagami- q	$(2, \frac{1+q}{1-q}, 0, 1, 1, 1)$
Nakagami- m	$(2, 1, 0, m, 1, 1)$
Weibull	$(\alpha, 1, 0, 1, 1, 1)$
60 GHz (LoS, indoor) [14]	$(3.49, 0.12, 0.6, 0.79, 0.5, 0.07)$
28 GHz (LoS, outdoor) [14]	$(2.2, 73, 5.7, 1.01, 1.05, 1)$
28 GHz (NLoS, outdoor) [14]	$(2.545, 0.006, 2.5, 1.98, 1.5, 1.05)$

components (namely, $p = q = 1$). However, the presence of imbalance between them are actually not uncommon in practical scenarios (e.g., the mmWave channels [14]), and the presence of channel imbalance also poses large impact on the effective throughput, which will be illustrated in later section.

It is also worth mentioning that since the sum of some specific RVs still exactly or approximately follows the distribution that can be well described by the $\alpha\text{-}\eta\text{-}\kappa\text{-}\mu$ model (e.g., the SNR caused by Nakagami- m fading [28] or $\alpha\text{-}\mu$ fading [29]), the obtained results on effective throughput for those fading distributions can be straightforwardly extended to the case with MISO or MIMO configurations. Thus, the derived results in (12) is very unified and generalized, which can be conveniently extended to various small-scale fading and antenna configuration. Following, based on the obtained analytical results for $\alpha\text{-}\eta\text{-}\kappa\text{-}\mu$ fading channel, we present the results on the effective throughput of a MIMO-OSTBC system over Rayleigh fading channels and a MISO system over Nakagami- m and $\alpha\text{-}\mu$ fading channels.

1) MIMO-OSTBC System over Rayleigh Fading

We first apply the aforementioned results for a MIMO system with orthogonal space-time block code (OSTBC) transmission over independent and quasi-static Rayleigh flat fading channels. The considered MIMO system is equipped with N_t transmitting antennas and N_r receiving antennas. The MIMO channel is represented by the matrix $\mathbf{H} = [h_{ij}]_{i,j=1}^{N_r, N_t}$ of $N_r \times N_t$ size with $h_{i,j}$ being the channel coefficient between the i -th receiving antenna and j -th transmitting antenna. Due to independent and identically distributed (i.i.d.) Rayleigh fading, the channel coefficients $h_{i,j}, i = 1, \dots, N_r, j = 1, \dots, N_t$, are i.i.d. complex circular Gaussian RVs, i.e., $h_{i,j} \sim \mathcal{CN}(0, 1)$. At the transmitter side, it selects R transmit symbols, which are encoded with a $N_t \times T$ OSTBC matrix \mathbf{Q} and transmitted over T time slots. The MIMO transmission is mathematically expressed as

$$\mathbf{Y} = \mathbf{H} \cdot \sqrt{P_T} \cdot \mathbf{Q} + \mathbf{W}, \quad (13)$$

where \mathbf{Y} is the received signal represented by $N_r \times T$ matrix, the $N_r \times T$ matrix \mathbf{W} models the receiver noise with elements being i.i.d. complex circular Gaussian RVs, i.e., each with distribution $\mathcal{CN}(0, \sigma^2)$, and P_T is the total transmit power per symbol time. Then, the average SNR per receiving antenna can be written as $\bar{\gamma}^{STBC} = \frac{P_T}{\sigma^2}$ [30]. It can be then obtained that the effective SNR at the receiver can be written as

$$\gamma^{STBC} = \frac{\bar{\gamma}^{STBC} \cdot \|\mathbf{H}\|_F^2}{R_c N_t}, \quad (14)$$

where R_c is the code rate.

Under the Rayleigh fading assumption, $\|\mathbf{H}\|_F^2$ is the sum of $2N_t N_r$ independent χ^2 RVs and is thus χ^2 -distributed with $2N_t N_r$ degrees of freedom [30]. Then, it is straightforward to show that the received SNR γ^{STBC} follows Gamma distribution with shape parameter $N_t N_r$. Finally, we can obtain the exact expression for the effective capacity

of MIMO system over i.i.d. Rayleigh channels as shown in (15) at the top of previous page, where the parameters in the bivariate Fox H-function are: $\mathcal{K}_{1a} = (1 - N_t N_r; 1, 1)$, $(\frac{1}{2} - N_t N_r; 1, 1)$; $\mathcal{K}_{1b} = (1 - N_t N_r; 1, 1)$; $\mathcal{K}_{2a} = (1 - A, 1)$; $\mathcal{K}_{2b} = (0, 1)$; $\mathcal{K}_{3a} = (1 - N_t N_r, 1)$; and $\mathcal{K}_{3b} = (0, 1)$, $(1 - N_t N_r, 1)$. It should be noted that the SNR $\bar{\gamma}$ in the expression (15) represents the mean of effective SNR in the above analysis, namely $E\{\gamma^{STBC}\} = \frac{N_r \bar{\gamma}^{STBC}}{R_c}$.

2) MISO System over Nakagami- m Fading

We consider a MISO communication system with N_t transmitting antennas and single receiving antenna. For tractability, the channel h_t , $t = 1, \dots, N_t$, between each transmitting antenna and receiving antenna are assumed to undergo i.i.d. Nakagami- m fading with the Nakagami shape parameter m . It is well-known that $|h_t|^2$ are Gamma distributed resulting from Nakagami fading and the sum of N_t i.i.d. Gamma RVs with shape parameters m_t is another Gamma RV with parameter $\sum_{t=1}^{N_t} m_t$ [31]. Therefore, the RV $s = \sum_{t=1}^{N_t} |h_t|^2$ is still Gamma distributed with shape parameter mN_t . Then, we can obtain the exact expression for the effective throughput of MISO system over i.i.d. Nakagami- m fading channel as shown in (16) at the top of previous page, where the parameters in the bivariate Fox H-function are: $\mathcal{K}_{1a} = (1 - mN_t; 1, 1)$, $(\frac{1}{2} - mN_t; 1, 1)$; $\mathcal{K}_{1b} = (1 - mN_t; 1, 1)$; $\mathcal{K}_{2a} = (1 - A, 1)$; $\mathcal{K}_{2b} = (0, 1)$; $\mathcal{K}_{3a} = (1 - mN_t, 1)$; and $\mathcal{K}_{3b} = (0, 1)$, $(1 - mN_t, 1)$.

3) MISO System over α - μ Fading

Again, we consider a MISO communication system with N_t transmitting antennas and one receiving antenna. The fading channel h_t , $t = 1, \dots, N_t$, across each pair of transmitting and receiving antenna are i.i.d. and follows the α - μ distribution. To evaluate the effective throughput for considered scenario, we need to know the statistics of the RV $s = \sum_{t=1}^{N_t} |h_t|^2$. It is generally difficult to obtain the exact statistics of the RV s . However, it is shown in [29] that for i.i.d. α - μ RVs $|h_t|$, the sum s can be well approximated by the PDF of squared channel gain of a single channel with parameters $\tilde{\alpha}$ and $\tilde{\mu}$. The values of the parameters $\tilde{\alpha}$ and $\tilde{\mu}$ can be obtained with the moment-based estimators detailed in [29, Eq. (22)–(24)]. Finally, the effective throughput of MISO system over i.i.d. α - μ fading channel can be obtained as shown in (17) at the top of previous page with the parameters in the H-function being: $\mathcal{K}_{1a} = (1 - \tilde{\mu}; \frac{2}{\tilde{\alpha}}, 1)$, $(\frac{1}{2} - \tilde{\mu}; \frac{2}{\tilde{\alpha}}, 1)$; $\mathcal{K}_{1b} = (1 - \tilde{\mu}; \frac{2}{\tilde{\alpha}}, 1)$; $\mathcal{K}_{2a} = (1 - A, 1)$; $\mathcal{K}_{2b} = (0, 1)$; $\mathcal{K}_{3a} = (1 - \tilde{\mu}, 1)$; and $\mathcal{K}_{3b} = (0, 1)$, $(1 - \tilde{\mu}, 1)$.

Also, since a number of small-scale fading distributions (i.e., exponential, Rayleigh, Gamma, Weibull, and Nakagami- m) are all special cases of the α - μ model [32], [33]. The effective throughput of multi-antenna systems over those small-scale fading channels can be straightforwardly obtained from the above results.

D. HIGH-SNR ANALYSIS

To gain more in-depth understandings on the impact of physical channel parameters as well as the system configuration on the effective throughput performance, we conduct the asymptotic analysis on the effective throughput by considering the high-SNR regime (i.e., $\bar{\gamma} \rightarrow \infty$) in this section.

We first investigate the effective throughput performance under the high-SNR regime when $\bar{\gamma} \rightarrow \infty$. Rewriting the exponential term in (7) using the Taylor series [23, Eq. (1.211)], the effective rate can be alternatively written as

$$\mathcal{R}(\bar{\gamma}, \theta) = -\frac{1}{A} \cdot \log_2 \left(\frac{\alpha \bar{\gamma}^{-\frac{\alpha\mu}{2}}}{2^{\mu+1} \Gamma(\mu)} \sum_{k=0}^{\infty} \frac{c_k}{(\mu)_k} \sum_{n=0}^{\infty} \frac{3^n \cdot \mathcal{J}}{(2\bar{\gamma}^{\frac{\alpha}{2}})^{n!}} \right), \quad (18)$$

where

$$\mathcal{J} = \int_0^{\infty} x^{\frac{\alpha\mu}{2} + \frac{\alpha n}{2} - 1} \cdot (1+x)^{-A} \cdot G_{1,2}^{1,1} \left(\frac{2x^{\frac{\alpha}{2}}}{\bar{\gamma}^{\frac{\alpha}{2}}} \middle| \begin{matrix} 1-k-\mu \\ 0, 1-\mu \end{matrix} \right) dx. \quad (19)$$

Again, using the equalities in (8) and the relationship in (10) to express the relevant terms in (19) into Fox H-functions and then solving the resultant integral with the aid of [20, Eq. (2.25.1)], the above integral \mathcal{J} can be solved as

$$\mathcal{J} = \frac{1}{\Gamma(A)} \cdot H_{2,3}^{2,2} \left(\frac{2}{\bar{\gamma}^{\frac{\alpha}{2}}} \middle| \begin{matrix} (1-k-\mu, 1), (1-\frac{\alpha\mu}{2}-\frac{\alpha n}{2}, \frac{\alpha}{2}) \\ (0, 1), (A-\frac{\alpha\mu}{2}-\frac{\alpha n}{2}, \frac{\alpha}{2}), (1-\mu, 1) \end{matrix} \right). \quad (20)$$

To obtain the asymptotic expression for the effective throughput when $\bar{\gamma} \rightarrow \infty$, we utilize the following asymptotic expression of Fox H-function [34, Cor. 2]:

$$\lim_{x \rightarrow 0} H_{p,q}^{s,t} \left(x \middle| \begin{matrix} (\mathbf{a}_p, \alpha_p) \\ (\mathbf{b}_q, \beta_q) \end{matrix} \right) \cong \sum_{j=1}^s \left[h_j \cdot x^{\frac{b_j}{\beta_j}} + \mathcal{O} \left(x^{\frac{b_j+1}{\beta_j}} \right) \right], \quad (21)$$

where

$$h_j = \frac{\prod_{i=1, i \neq j}^s \Gamma(b_i - \frac{b_j \beta_i}{\beta_j}) \cdot \prod_{i=1}^t \Gamma(1 - a_i + \frac{b_j a_i}{\beta_j})}{\beta_j \cdot \prod_{i=t+1}^p \Gamma(a_i - \frac{b_j a_i}{\beta_j}) \cdot \prod_{i=s+1}^q \Gamma(1 - b_i + \frac{b_j \beta_i}{\beta_j})}. \quad (22)$$

Using the above asymptotic relationship of Fox H-function in (21)–(22) for the H-function in (20), we can obtain the asymptotic expression of the effective throughput at high SNR as

$$\mathcal{R}^{\infty} \cong -\frac{1}{A} \cdot \log_2 \left(\frac{\alpha}{2^{\mu+1} \Gamma(\mu) \Gamma(A) \bar{\gamma}^{\frac{\alpha\mu}{2}}} \cdot \sum_{k=0}^{\infty} \frac{c_k}{(\mu)_k} \cdot \left(1 + \frac{3}{2\bar{\gamma}^{\frac{\alpha}{2}}} \right) \cdot \left[h_1 + h_2 \left(\frac{2}{\bar{\gamma}^{\frac{\alpha}{2}}} \right)^{\frac{2A}{\alpha} - \mu} \right] \right), \quad (23)$$

where the terms h_1 and h_2 can be simply calculated from the expression in (22).

As the asymptotic effective throughput is dominated by the lowest power of the $\bar{\gamma}$ in (23), we can continue to obtain that

TABLE 2. High-SNR Slope S^∞ for Some Conventional Fading Distributions Based on Effective Throughput Analysis for α - η - κ - μ Fading Channel

Fading	S^∞	Fading	S^∞
α - μ	$\min(1, \frac{\alpha\mu}{2A})$	Rayleigh	$\min(1, \frac{1}{A})$
κ - μ	$\min(1, \frac{\mu}{A})$	Rician	$\min(1, \frac{1}{A})$
Beckmann	$\min(1, \frac{1}{A})$	Nakagami- q	$\min(1, \frac{1}{A})$
Nakagami- m	$\min(1, \frac{m}{A})$	Weibull	$\min(1, \frac{\alpha}{2A})$

when $\frac{2A}{\alpha} - \mu > 0$ holds, the asymptotic throughput can be further simplified as

$$\begin{aligned} \mathcal{R}^\infty &\cong -\frac{1}{A} \cdot \log_2 \left(\frac{\alpha \Gamma(A - \frac{\alpha\mu}{2}) \Gamma(\frac{\alpha\mu}{2})}{2^{\mu+1} [\Gamma(\mu)]^2 \Gamma(A) \bar{\gamma}^{\frac{\alpha\mu}{2}}} \cdot \sum_{k=0}^{\infty} \frac{c_k \Gamma(k + \mu)}{(\mu)_k} \right) \\ &\cong -\frac{1}{A} \cdot \log_2 \left(\frac{\alpha \cdot B(A - \frac{\alpha\mu}{2}, \frac{\alpha\mu}{2})}{2^{\mu+1} \Gamma(\mu) \bar{\gamma}^{\frac{\alpha\mu}{2}}} \cdot \sum_{k=0}^{\infty} c_k \right). \end{aligned} \quad (24)$$

Following the same rationale, the asymptotic effective throughput in the case of $\frac{2A}{\alpha} - \mu < 0$ can be written as

$$\mathcal{R}^\infty \cong -\frac{1}{A} \cdot \log_2 \left(\frac{\alpha 2^{\frac{2A}{\alpha} - \mu}}{2^{\mu+1} \Gamma(\mu) \Gamma(A) \bar{\gamma}^A} \cdot \sum_{k=0}^{\infty} \frac{c_k}{(\mu)_k} \cdot h_2 \right). \quad (25)$$

It is clear from (24) and (25) that the high-SNR slope defined as $S^\infty = \frac{\mathcal{R}^\infty}{\log_2 \bar{\gamma}}$ is $\frac{\alpha\mu}{2A}$ when $A \geq \frac{\alpha\mu}{2}$ and the high-SNR slope is 1 when $A < \frac{\alpha\mu}{2}$. Then, we can conclude that for α - η - κ - μ fading channels, the value of the high-SNR slope is given by

$$S^\infty = \begin{cases} \frac{\alpha\mu}{2A} & A \geq \frac{\alpha\mu}{2}, \\ 1 & A < \frac{\alpha\mu}{2}. \end{cases} \quad (26)$$

Observing (26), it is obvious that the high-SNR slope S^∞ is independent of the SNR and is only determined by the channel characteristics and the parameter A . More specifically, the high-SNR slope is only dependent on the channel nonlinearity and the number of multipath clusters when $A \geq \frac{\alpha\mu}{2}$. This is in accordance with the conclusions on the high-SNR slopes for the Nakagami- m fading channel in [25, Eq. (30)] and the Rayleigh fading channel in [35, Eq. (16)], where both the Nakagami- m and Rayleigh fading are special cases of the α - η - κ - μ fading model.

A summary of the high-SNR slope S^∞ for some widely used conventional fading distributions is given in Table 2 at the top of this page. Interestingly, it can be observed from Table 2 that for a wide range of fading distributions (e.g., Rayleigh, Rician, Beckmann, and Nakagami- q distributions), the value of the high-SNR slope is independent of the channel parameters but only depends on the parameter $A = \frac{\theta TB}{\ln 2}$. When $A \leq 1$ holds, the aforementioned fading distributions will all have the high-SNR slope value of 1.

III. NUMERICAL RESULTS AND DISCUSSIONS

In this section, we evaluate the effective throughput performance of the α - η - κ - μ fading channels with varying physical channel parameters and system configurations.

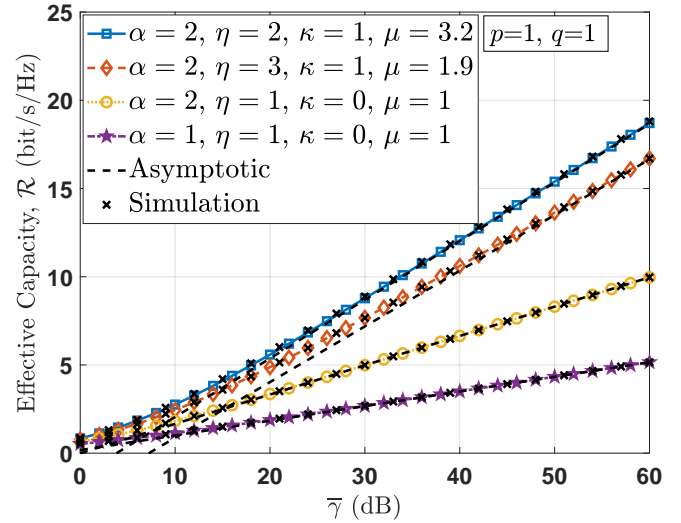


FIGURE 2. Effective throughput with different values of α and μ , $A = 2$

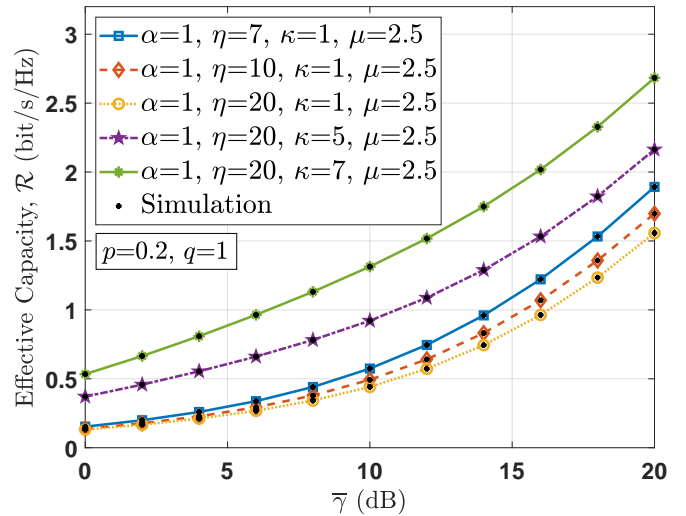


FIGURE 3. Effective throughput with different values of η and κ , $A = 1$

Figure 2 shows the effective throughput as a function of the average SNR $\bar{\gamma}$ with asymptotic curves. It can be seen that the effective throughput improves with the increase of channel nonlinearity and number of multipath clusters. The asymptotic curves of the effective throughput are also in accordance with the conducted analysis in high-SNR analysis (note that the derived high-SNR slope $\frac{\alpha\mu}{2A}$ is not equal to the slope of asymptotic curves in Figure 2 that is plotted against $10 \log_{10} \bar{\gamma}$). For further verification of the conclusion in Eq. (26), we first check the case when $\alpha = 2, \eta = 2, \kappa = 1$, and $\mu = 3.2$, the effective capacity at the SNR of 60 dB is 18.8 bits/s/Hz while it is 15.34 bits/s/Hz at the SNR of 50 dB. Thus, the slope of the asymptotic curve over 10 dB is $(18.7094 - 15.3884) * \log_{10} 2 = 0.9997 \approx 1$, which verifies the asymptotic slope derived analytically in Eq. (26) for the case of $A < \frac{\alpha\mu}{2}$. Let us then verify the asymptotic slope when $A > \frac{\alpha\mu}{2}$. We observe from Figure 2 that when $\alpha = 2$,

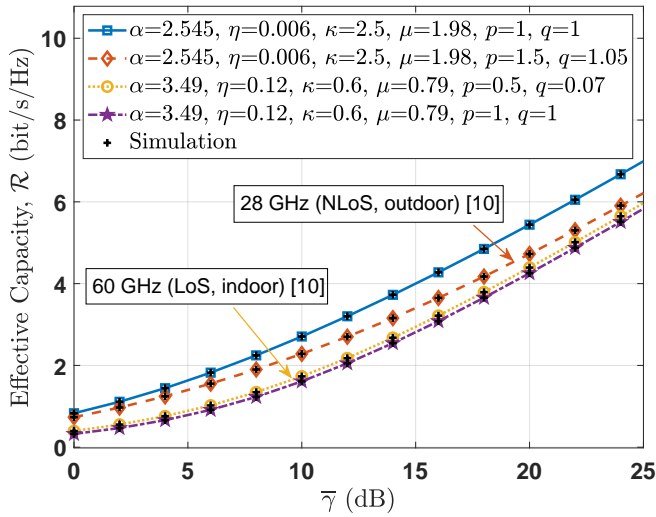


FIGURE 4. Effective throughput with different values of p and q , $A = 2$

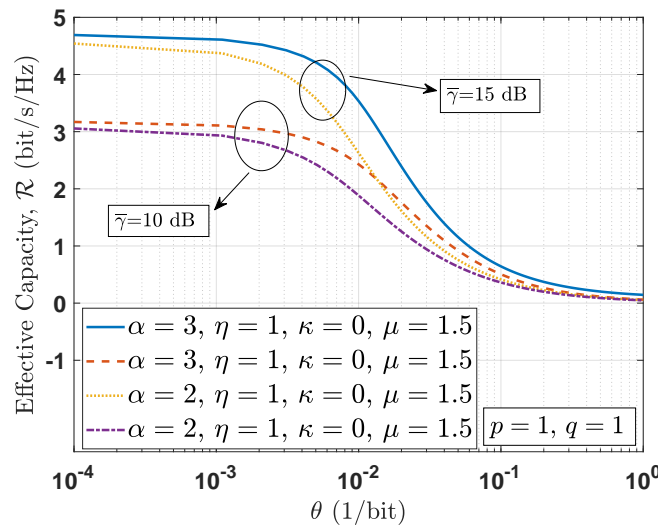


FIGURE 5. Effective throughput versus the QoS exponent parameter θ

$\eta = 1$, $\kappa = 0$, and $\mu = 1$, the effective capacity values at the SNRs of 50 dB and 60 dB are, respectively, 8.305 and 9.966 bits/s/Hz. Thus, the slope of the asymptotic curve over 10 dB is $(9.966 - 8.305) * \log_{10} 2 = 0.5 = \frac{\alpha\mu}{2A}$, which again verifies the asymptotic slope derived analytically in Eq. (26). Please note that the $\log_{10} 2$ factor is present because the asymptotic slope for (24) and (25) are defined in terms of $\log_2 \bar{\gamma}$ (that is base 2 in the logarithm), while the curves we have plotted have $\bar{\gamma}$ in dB on the x-axis (that is base 10 in the logarithm).

Figure 3 illustrates the impact of parameters η and κ on the effective throughput. It is obvious that lower values of η imply higher effective throughput while the opposite is true for κ . The effect of parameter κ implies that when the total power is fixed, smaller scattered power can improve the effective throughput. The results on η indicate that the power of in-phase and quadrature scattered waves of the multipath clusters also have different impacts on effective

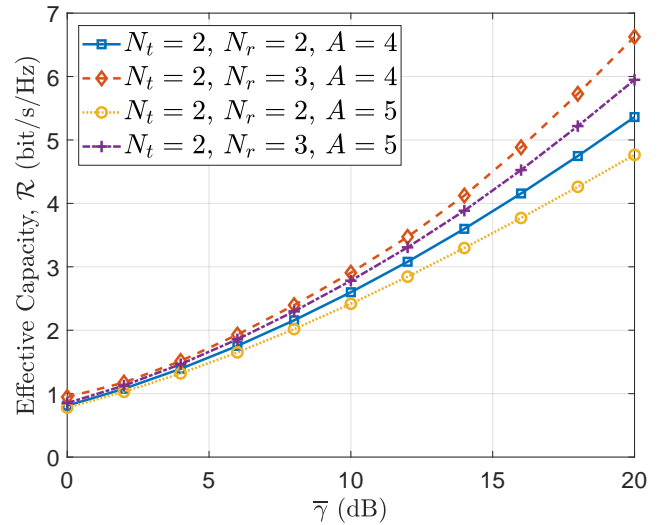


FIGURE 6. Effective throughput of MIMO system over Rayleigh channels

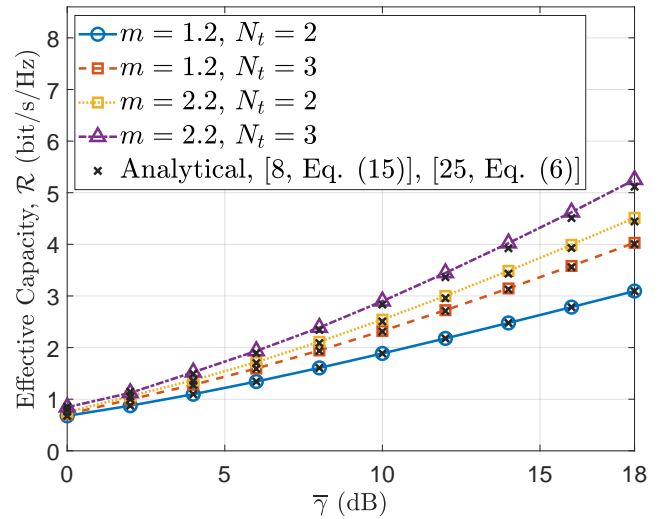


FIGURE 7. Effective throughput of MISO system over Nakagami channels, $A = 5$

throughput, where the lower ratio of in-phase scattered power indicates larger effective throughput. The impacts of in-phase and quadrature wave powers on effective throughput is also in accordance with the results in Figure 4, which shows the influence of channel imbalance of mmWave channels on effective throughput. It can be seen from Figure 4 that as the value of the channel imbalance parameters p and q decrease, the effective throughput improves. It is also interesting to observe from Figure 4 that the NLoS outdoor mmWave channel at 28 GHz exhibits larger effective throughput than the LoS scenario of 60 GHz indoor channel under the same average SNR (i.e., without considering the effect of path loss).

The effective throughput versus the QoS exponent θ is plotted in Figure 5. Overall, the results show that the effective throughput performance degrades upon a larger QoS exponent θ , which implies that as the delay constraints be-

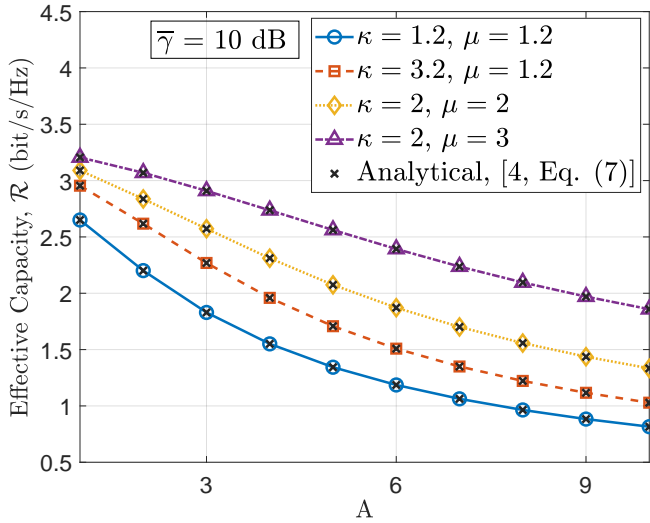


FIGURE 8. Impact of A on effective throughput over κ - μ channels, $\bar{\gamma} = 10$ dB

come larger, the less effective throughput the system can handle. However, it is also seen that when the QoS exponent is sufficiently small, increasing θ within the corresponding region can only pose slight impact on the effective throughput performance; and the effective throughput performance degrades significantly with the increase of QoS exponent after θ grows larger than some threshold.

Figure 6 illustrates the effective throughput of the MIMO system over Rayleigh fading channel in terms of average SNR with the help of results in Sec. II-C1. It is clear that the effective capacity improves with the increase of number of antennas in the MIMO system, which is in accordance with the results in [36]. The effective throughput against the average SNR for the MISO system over the Nakagami- m fading channels by utilizing the results in Sec. II-C2 is shown in Figure 7. The simulation results in Figure 7 are also in accordance with the results obtained by the analytical expressions in [8, Eq. (15)] and [25, Eq. (6)] despite they are in different forms. The impact of the parameter A on the effective throughput is demonstrated in Figure 8, which is in agreement with results from the theoretical expressions in [4, Eq. (7)]. The results obviously demonstrate the generality and flexibility of the analysis on α - η - κ - μ fading channels.

IV. CONCLUSION

In this paper, we studied the effective throughput performance of the α - η - κ - μ fading channels by deriving the general and exact analytical expression of effective throughput and by conducting asymptotic analysis for the effective throughput at high-SNR regime. The obtained results implicitly reveal the impact of different physical channel characteristics on the effective throughput performance. The derived expressions are highly general and can be widely used for various practical channels (e.g., mmWave channels, etc.) and various configurations (e.g., MISO, MIMO, etc.).

REFERENCES

- [1] D. Wu and R. Negi, "Effective capacity: a wireless link model for support of quality of service," *IEEE Trans. Wireless Commun.*, vol. 2, no. 4, pp. 630–643, Jul. 2003.
- [2] M. Amjad, L. Musavian, and M. H. Rehmami, "Effective capacity in wireless networks: A comprehensive survey," *IEEE Commun. Surveys Tuts.*, vol. 21, no. 4, pp. 3007–3038, Jul. 2019.
- [3] Q. Wang, D. Wu, and P. Fan, "Effective capacity of a correlated Rayleigh fading channel," *Wireless Commun. Mobile Comput.*, vol. 11, no. 11, pp. 1485–1494, Nov. 2011.
- [4] J. Zhang, Z. Tan, H. Wang, Q. Huang, and L. Hanzo, "The effective throughput of MISO systems over κ - μ fading channels," *IEEE Trans. Veh. Technol.*, vol. 63, no. 2, pp. 943–947, Feb. 2013.
- [5] F. Almechadi and O. Badarneh, "On the effective capacity of Fisher-Snedecor \mathcal{F} fading channels," *Electron. Lett.*, vol. 54, no. 18, pp. 1068–1070, Sept. 2018.
- [6] H. Al-Hmood and H. S. Al-Raweshidy, "Unified approaches based effective capacity analysis over composite α - η - μ /gamma fading channels," *Electron. Lett.*, vol. 54, no. 13, pp. 852–853, Jun. 2018.
- [7] M. You, H. Sun, J. Jiang, and J. Zhang, "Unified framework for the effective rate analysis of wireless communication systems over MISO fading channels," *IEEE Trans. Commun.*, vol. 65, no. 4, pp. 1775–1785, Apr. 2017.
- [8] J. Zhang, L. Dai, Z. Wang, D. W. K. Ng, and W. H. Gerstacker, "Effective rate analysis of MISO systems over α - μ fading channels," in *Proc. IEEE Global Commun. Conf. (GLOBECOM)*. San Diego, CA, USA: IEEE, Dec. 2015, pp. 1–6.
- [9] W. Cheng, X. Zhang, and H. Zhang, "QoS-aware power allocations for maximizing effective capacity over virtual-MIMO wireless networks," *IEEE J. Sel. Areas Commun.*, vol. 31, no. 10, pp. 2043–2057, Oct. 2013.
- [10] C. Xiao, J. Zeng, W. Ni, R. P. Liu, X. Su, and J. Wang, "Delay guarantee and effective capacity of downlink NOMA fading channels," *IEEE J. Sel. Topics Signal Process.*, vol. 13, no. 3, pp. 508–523, Jun. 2019.
- [11] M. Shehab, H. Alves, and M. Latva-aho, "Effective capacity and power allocation for machine-type communication," *IEEE Trans. Veh. Technol.*, vol. 68, no. 4, pp. 4098–4102, Apr. 2019.
- [12] G. Femenias, J. Ramis, and L. Carrasco, "Using two-dimensional markov models and the effective-capacity approach for cross-layer design in AMC/ARQ-based wireless networks," *IEEE Trans. Veh. Technol.*, vol. 58, no. 8, pp. 4193–4203, Oct. 2009.
- [13] M. D. Yacoub, "The α - η - κ - μ fading model," *IEEE Trans. Antennas Propag.*, vol. 64, no. 8, pp. 3597–3610, Aug. 2016.
- [14] A. A. dos Anjos, T. R. R. Marins, R. A. A. de Souza, and M. D. Yacoub, "Higher order statistics for the α - η - κ - μ fading model," *IEEE Trans. Antennas Propag.*, vol. 66, no. 6, pp. 3002–3016, Jun. 2018.
- [15] A. Mathur, Y. Ai, M. R. Bhatnagar, M. Cheffena, and T. Ohtsuki, "On physical layer security of α - η - κ - μ fading channels," *IEEE Commun. Lett.*, vol. 22, no. 10, pp. 2168–2171, Oct. 2018.
- [16] Y. Ai, M. Cheffena, A. Mathur, and H. Lei, "On physical layer security of double Rayleigh fading channels for vehicular communications," *IEEE Wireless Commun. Lett.*, vol. 7, no. 6, pp. 1038–1041, Dec. 2018.
- [17] V. M. Rennó, R. A. de Souza, and M. D. Yacoub, "On the generation of α - η - κ - μ samples with applications," in *Proc. IEEE Annu. Int. Symp. Pers., Indoor, Mobile Radio Commun. (PIMRC)*. Montreal, Canada: IEEE, Oct. 2017, pp. 1–5.
- [18] Y. Ai, L. Kong, and M. Cheffena, "Secrecy outage analysis of double shadowed Rician channels," *Electron. Lett.*, vol. 55, no. 13, pp. 765–767, Jun. 2019.
- [19] X. Li, X. Chen, J. Zhang, Y. Liang, and Y. Liu, "Capacity analysis of α - η - κ - μ fading channels," *IEEE Commun. Lett.*, vol. 21, no. 6, pp. 1449–1452, Jun. 2017.
- [20] A. Prudnikov, Y. Brychkov, and O. Marichev, *Integrals and Series. Volume 3: More Special Functions*. New York, NY, USA: Gordon and Breach Sci. Publ., 1986.
- [21] A. M. Mathai, R. K. Saxena, and H. J. Haubold, *The H-function: Theory and Applications*. Berlin, Germany: Springer Science & Business Media, 2009.
- [22] K. P. Peppas, "A new formula for the average bit error probability of dual-hop amplify-and-forward relaying systems over generalized shadowed fading channels," *IEEE Wireless Commun. Lett.*, vol. 1, no. 2, pp. 85–88, Apr. 2012.
- [23] I. S. Gradshteyn and I. M. Ryzhik, *Table of Integrals, Series, and Products*, 7th ed. Burlington, MA, USA: Academic Press, 2007.

- [24] A. J. Laub, *Matrix Analysis for Scientists and Engineers*. Philadelphia, PA, USA: SIAM, 2005, vol. 91.
- [25] M. Matthaiou, G. C. Alexandropoulos, H. Q. Ngo, and E. G. Larsson, "Analytic framework for the effective rate of MISO fading channels," *IEEE Trans. Commun.*, vol. 60, no. 6, pp. 1741–1751, Jun. 2012.
- [26] X. Li, J. Li, L. Li, J. Jin, J. Zhang, and D. Zhang, "Effective rate of MISO systems over κ - μ shadowed fading channels," *IEEE Access*, vol. 5, pp. 10 605–10 611, Mar. 2017.
- [27] P. Mittal and K. Gupta, "An integral involving generalized function of two variables," in *Proc. Indian Acad. Sci.-Sec. A*, vol. 75, no. 3. Springer, Mar. 1972, pp. 117–123.
- [28] M. K. Simon and M.-S. Alouini, *Digital Communication over Fading Channels*. New York, NY, USA: John Wiley & Sons, 2005, vol. 95.
- [29] D. B. Da Costa, M. D. Yacoub, and J. C. S. S. Filho, "Highly accurate closed-form approximations to the sum of α - μ variates and applications," *IEEE Trans. Wireless Commun.*, vol. 7, no. 9, pp. 3301–3306, Sept. 2008.
- [30] A. Maaref and S. Aissa, "Shannon capacity of STBC in Rayleigh fading channels," *Electron. Lett.*, vol. 40, no. 13, pp. 817–819, Jun. 2004.
- [31] Y. Ai and M. Cheffena, "On multi-hop decode-and-forward cooperative relaying for industrial wireless sensor networks," *Sensors*, vol. 17, no. 4, p. 695, Mar. 2017.
- [32] M. D. Yacoub, "The α - μ distribution: A physical fading model for the Stacy distribution," *IEEE Trans. Veh. Technol.*, vol. 56, no. 1, pp. 27–34, Jan. 2007.
- [33] A. Mathur, Y. Ai, M. Cheffena, and G. Kaddoum, "Secrecy performance of correlated α - μ fading channels," *IEEE Commun. Lett.*, vol. 23, no. 8, pp. 1323–1327, Aug. 2019.
- [34] A. A. Kilbas and M. Saigo, "On the H-function," *J. Appl. Math. Stoch. Anal.*, vol. 12, no. 2, pp. 191–204, Sept. 1999.
- [35] C. Zhong, T. Ratnarajah, K.-K. Wong, and M.-S. Alouini, "Effective capacity of correlated MISO channels," in *Proc. IEEE Int. Conf. Commun. (ICC)*. Kyoto, Japan: IEEE, Jul. 2011, pp. 1–5.
- [36] X. Li, L. Li, X. Su, Z. Wang, and P. Zhang, "Approximate capacity analysis for distributed MIMO system over generalized-K fading channels," in *Proc. IEEE Wireless Commun. Netw. Conf. (WCNC)*. New Orleans, LA, USA: IEEE, Mar. 2015, pp. 235–240.

...